Process-Property-Performance Relationships for Titanium Dioxide Coatings Engineered from Nanostructured and Conventional Powders

Lima, Rogerio; Marple, Basil

Publisher's version / Version de l'éditeur:
http://dx.doi.org/10.1016/j.matdes.2008.03.005
Materials and Design, 29, 9, pp. 1845-1855, 2008

Materials and Design 29 (2008) 1845–1855

Contents lists available at ScienceDirect

Materials and Design

journal homepage: www.elsevier.com/locate/matdes

Process–property–performance relationships for titanium dioxide coatings engineered from nanostructured and conventional powders

R.S. Lima *, B.R. Marple

National Research Council of Canada, 75 de Mortagne Blvd., Boucherville, QC, Canada J4B 6Y4

ARTICLE INFO

Article history:
Received 4 January 2008
Accepted 13 March 2008
Available online 21 March 2008

Keywords:
Thermal spray coating
Nanostructured titania (TiO_2) powder
Dry-sliding wear
Microstructure
Processing

ABSTRACT

Nanostructured (Nano), fused and crushed (F&C) and plasma-fused (PF) titania (TiO_2) powder particles were thermally sprayed via flame spray (FS), air plasma spray (APS) and high velocity oxy-fuel (HVOF) on low carbon steel substrates. Flame spray processing, although widely employed industrially, generally has received very limited attention in academic papers. However, the results of this research have demonstrated that a FS Nano titania coating was the best performing among all coatings tested, exhibiting no measurable signs of mass/volume loss after dry-sliding wear testing (ball-on-disk) and the highest deposition efficiency (DE) level. This is regarded as an important result, considering the fact that among these three processing techniques FS is the least expensive, the most portable and exhibits the lowest energy consumption levels. In addition, scanning electron microscopy (SEM) analysis demonstrated that the sliding wear scars of the FS and HVOF-sprayed Nano coatings were smooth, without significant irreversible deformation or formation of ridges. These characteristics are not typical of ceramic materials. It is hypothesized that this plastic-like behaviour and resilience exhibited by FS and HVOF-sprayed Nano coatings explain their improved performance under dry-sliding wear.

1. Introduction

1.1. Titania coatings and nanostructured-based powders

Titania (TiO_2) thermal spray coatings are recommended for anti-wear applications involving hard surfaces (sliding wear) and abrasive grains [1]. As examples to be cited, titania coatings have been applied to pump seals and bearing surfaces [2]. Nanostructured and/or ultrafine materials offer the potential for significant improvement in the structural properties of materials, including coatings for anti-wear applications. In fact, it has been observed by different researchers that thermal spray coatings produced from nanostructured-based powders exhibit enhanced wear resistance when compared to coatings produced from other types of powders [3,4].

The most widely employed thermal spray processing techniques to deposit ceramic-based feedstock materials in the powder form are air plasma spray (APS), high velocity oxy-fuel (HVOF) and flame spray (FS). Of these, FS processing is not often the focus of scientific papers; however, it is a successful processing technique in the thermal spray industry. It must be pointed out that FS processing is the most affordable and portable and exhibits the lowest energy consumption levels of the techniques previously cited. Therefore, it would be interesting to verify if significant gains in anti-wear properties could be observed by combining FS processing with nanostructured-based powders.

1.2. Influence of the nanostructural character of the powder on the structural properties of the coatings

Despite the fact that enhanced anti-wear properties have been observed for ceramic thermal spray coatings produced from nanostructured-based powders [3,4], there is still some controversy on the role of the nanostructured character of the powder feedstock on the mechanical performance of the coatings. One way to investigate this phenomenon is to produce a feedstock powder that exhibits nanostructured and/or ultrafine character and try to "destroy" the nanostructure by passing them through a high temperature plasma (high melting) to form plasma-fused (PF) powder particles. After being fused (i.e., its major nanostructural character suppressed), the PF particles then would be thermally sprayed to form coatings, which would be compared to coatings produced from nanostructured-based powders.

The objective of this work was to carry out this experiment and compare the dry-sliding wear behaviour of coatings produced from nanostructured, fused and crushed and PF particles deposited via APS, HVOF and FS processing.

* Corresponding author. Tel.: +1 450 641 5150; fax: +1 450 641 5105.
E-mail address: rogerio.lima@cnrc-nrc.gc.ca (R.S. Lima).

0261-3069/$ - see front matter
doi:10.1016/j.matdes.2008.03.005

2. Experimental procedure

2.1. Powder and processing

All torches and powders employed in this study were furnished by one supplier (Sulzer Metco (US) Inc., Westbury, NY, USA). Information on these torches and powders can be found in Table 1. Argon (Ar) and hydrogen (H_2) were the plasma gases used with the APS torch. The HVOF and FS torches employed propylene and acetylene as fuel gases, respectively. Three types of titania powders were used in this study to produce coatings: nanostructured (Nano), fused and crushed (F&C) and plasma-fused (PF). Concerning the PF powder, as mentioned in Section 1.2, an experimental spray-dried titania powder with ultrafine structure (which was not used to produce coatings), was manufactured and subsequently fused via plasma, forming the PF powder particles.

The particle size distribution was evaluated by using a laser diffraction particle size analyzer (Beckman Coulter LS 13320, Beckman Coulter, Miami, FL, USA). All coatings were deposited on low carbon steel substrates. The coating thicknesses were approximately 500–600 μm.

The sprayed particles (in some cases) had their velocities and temperature values measured via one of two types of in-flight diagnostic tools (DPV 2000 or Accuraspray, Tecnar Automation, Saint Bruno, QC, Canada). Both types of equipment are based on pyrometry and time-of-flight measurements. The particle detector was placed at the same spray distance as used when depositing the coatings.

2.2. Powder morphology and microstructural evaluation

The structural characteristics of the powders, the cross-sections and the sliding wear tracks of the coatings were evaluated by field-emission scanning electron microscopy (FE-SEM) (Model S4700, Hitachi Instruments Inc., Tokyo, Japan). In order to better preserve and reveal the true structural features of the coatings (cross-section), they were mounted in epoxy resin using vacuum impregnation and polished using standard metallographic procedures. The porosity of the coatings was evaluated by using SEM and image analysis on the cross-sections. A total of 10 pictures of each coating was taken (at 500×) to evaluate the respective porosity levels. In order to ensure uniformity of porosity measurements, (i) the pictures of the cross-sections of all coatings were taken at the same SEM conditions and (ii) during image analysis the porosity levels of all coatings were evaluated using the same threshold levels.

2.3. Microhardness and crack propagation resistance

Vickers microhardness measurements were performed under a 300 gf load for 15 s on the polished cross-section of the coatings. A total of 10 microhardness measurements were carried out for each coating.

The crack propagation resistance was determined by indenting the coating cross-sections (in the centerline of the coating microstructure) with a Vickers indenter at a 1 kgf load for 15 s, with the indenter aligned such that one of its diagonals would be parallel to the substrate surface. The total length (tip-to-tip) of the major crack ($2c$) parallel to the substrate surface that originated at or near the corners of the Vickers indentation impression was measured. Based on the indentation load (P) and $2c$, the crack propagation resistance was calculated according to the relation between load and crack length, $P/c^{3/2}$, where P is in Newtons and c is in meters [5]. A total of 10 indentations were carried out for each coating.

It is important to point out that the crack propagation resistance concept applied in this study is not an absolute measure of fracture toughness. To determine indentation fracture toughness other parameters, such as hardness and elastic modulus, must be introduced in the calculation. However, crack propagation resistance is a useful technique to compare coatings that (i) exhibit similar porosity and thickness levels and (ii) were deposited using the same type of thermal spray processing. It provides a basis for determining the relative effect of the thermal spray processing and powder morphology on crack propagation characteristics and wear performance.

2.4. Dry-sliding wear testing

Ball-on-disk dry-sliding tests were performed at room temperature and atmosphere conditions on a micro tribometer (UMT-2, CETR, Mountain View, CA, USA) by using a ruby ball (diameter: 10 mm) on titania-coated, disk-shaped (radius: 3 cm), low carbon steel substrates. It has been cited that alumina-based materials (e.g., ruby – Mohs hardness scale 9) are chosen as a counterface material because they tend to exhibit a high coefficient of friction against coatings in dry-sliding, thereby promoting accelerated wear, which is measurable in the timescale of a laboratory testing exercise [6,7]. Bolelli et al. hypothesized that a high coefficient of friction would tend to be generated between the alumina-based balls and oxide coatings due to chemical affinity [8]. The coated substrates were fixed to a rotating disk, whereas, the ruby ball was fixed into a stationary ball holder pressed against the coating surface with a normal load of 30 N. The radius of the travelling circle of the ball on the disk was 2.4 cm. The total sliding distance and linear sliding speed values were 300 m and 5 cm/s, respectively. The surfaces of the titania coatings were ground and polished before wear testing, and exhibited roughness (R_a) values of approximately 0.10 μm. After each wear test, the ruby ball was carefully examined and its position changed to provided a new undamaged counterface contact at the start of each new wear trial.

The loss of material was determined by weighing the samples before and after the test. The mass loss values were converted to volume loss values by measuring the densities of free-standing titania coatings (that had been removed from the low carbon steel substrates by dissolving the metal base) via the geometrical method, except the F&C APS coating, for which the density value was obtained from the coating manufacturer's technical bulletin [2]. The density range was 3.8–4.1 g/cm^3. One sliding test per sample was performed.

Table 1
Titania powder, particle size distribution (in volume), morphology and torches employed in this study to produce coatings for wear testing

Powder	d_{10} (μm)	d_{50} (μm)	d_{90} (μm)	APS torch	HVOF torch	FS torch
F&C	15	32	51	9 MB	DJ2700-hybrid	6P-II
PF	10	20	32	9 MB	DJ2700-hybrid	–
Nano	18	27	38	9 MB	DJ2700-hybrid	6P-II

3. Results and discussion

3.1. Titania powders

Fig. 1a shows an experimental ultrafine titania powder produced via spray-drying. When the powder is observed at higher magnifications it is possible to distinguish its ultrafine structure (Fig. 1b), exhibiting particles with diameters varying from ~40 to 150 nm. It is important to stress that this powder was not thermally sprayed to produce coatings. As previously stated in Section 2.1, this powder was plasma-fused to form PF particles (Fig. 2a), which led to a loss of part of the original ultrafine character in the resulting feedstock (Fig. 2b).

Fig. 3 shows the F&C particle. It is possible to observe the typical irregular and blocky morphology of these types of particles and the absence of an ultrafine character.

Fig. 4 shows the nanostructured titania feedstock powder formed via spray-drying. It exhibits the typical "donut shape" of spray-dried particles. When observed at higher magnification, it is possible to distinguish the nanostructural character of the feedstock, i.e., the individual particles are smaller than 100 nm.

3.2. In-flight particle characteristics

Table 2 shows the in-flight particle characteristics and deposition efficiency (DE) values measured for some of the coatings produced in this study. The melting point of titania is 1855 °C [9]; therefore, by looking at Table 2, it is possible to observe that for all powders the average particle surface temperature was higher than this value. Because the particle temperatures were measured via a pyrometer, the temperatures reported represent only those at the particle surface, i.e., inner particle temperature levels may be lower or higher than the values given in Table 2. It also must be noted that the values shown in the table are the average values; i.e., the particles in the spray jet exhibited a range of temperatures.

Due to the low DE value of the HVOF-sprayed F&C coating, further analysis was not carried out for this coating. This low DE value is probably related to the particle size distribution of the powder. The F&C powder exhibited the largest fraction of large particles (i.e., highest d_{90}) among the three powders HVOF-sprayed (Table 1). The larger particles probably exhibited no or a somewhat limited degree of melting during HVOF-spraying. This impeded them from adhering on the coating surface and probably caused them to behave as hot grit-blasters, lowering substantially the DE values. Previous studies have observed that for obtaining "optimized" coatings during HVOF-spraying of pure ceramic oxides (e.g., TiO_2,

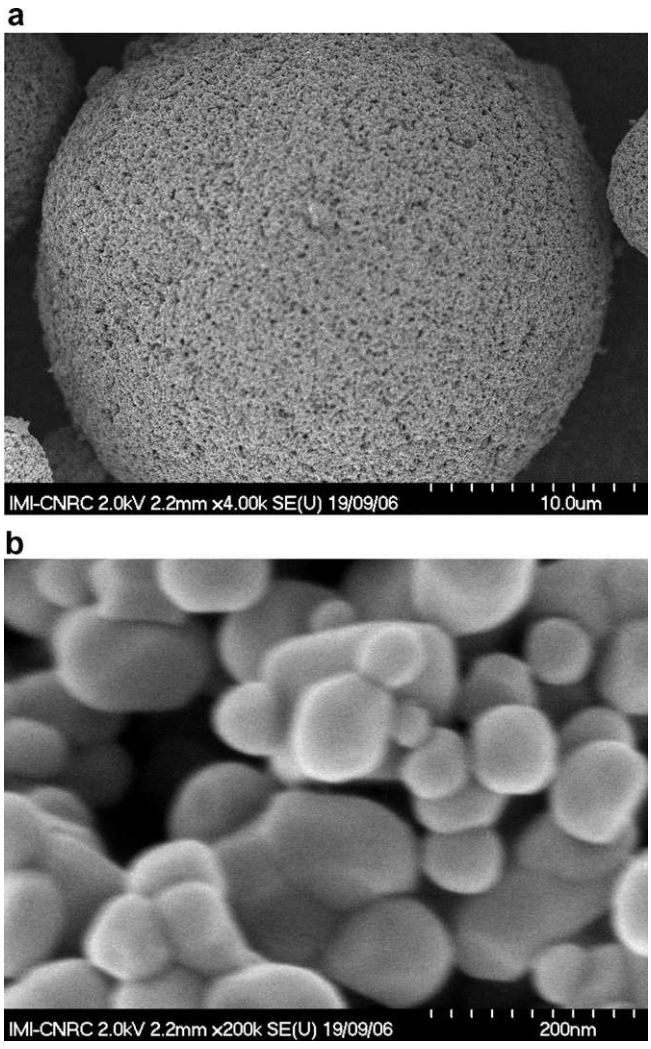

Fig. 1. (a) Experimental spray-dried titania ultrafine powder that was subsequently plasma-fused. (b) Higher magnification view of (a) showing the ultrafine structure, i.e., individual particles with diameters varying from 40 to 150 nm.

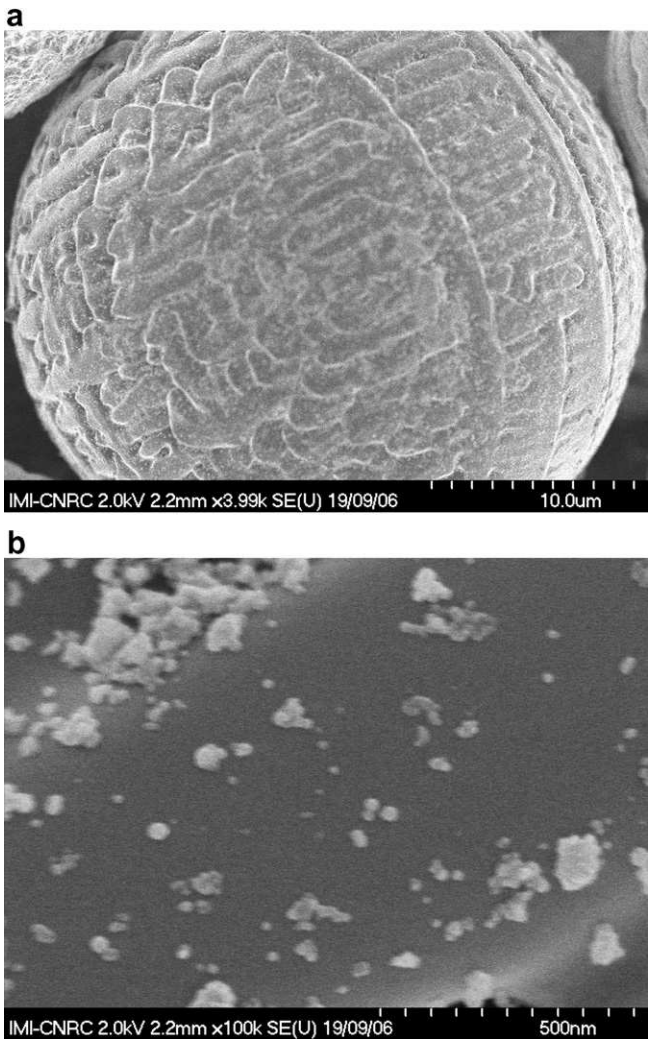

Fig. 2. (a) Spray-dried titania powder of Fig. 1 after being plasma-fused (PF). (b) Higher magnification view of (a) showing the absence of the ultrafine character after the plasma-fusing process.

Al_2O_3 and Cr_2O_3), particle size ranges from about 5 to 25 μm had to be employed [10–14]. However, as shown in the next sections, HVOF-sprayed Nano and PF particles exhibited dense and uniform microstructures, despite the fact that particles larger than the 5–25 μm distribution were employed (Table 1).

The DE value of the FS Nano coating stands out, reaching a value of approximately 80%. This is an important observation, regarding the fact FS systems are widely used in thermal spray job shops.

3.3. Coating microstructure and porosity

Fig. 5 shows the microstructures (cross-sections) of the titania coatings produced via FS processing. The coating made from the F&C powder (Fig. 5a) exhibits pore sizes varying from a few microns up to 20 μm. The FS coating made from the Nano powder exhibits a more uniform microstructure, with an even distribution of smaller pores (Fig. 5b). The porosity level of the Nano coating is slightly lower than that of the F&C one (Table 3).

Fig. 6 shows the microstructures (cross-sections) of the titania coatings produced via HVOF processing. Both coatings exhibit similar microstructural features, such as, the absence of a lamellar structure, even distribution of small pores and no significant microcracking. The porosity level of both coatings is approximately 1% (Table 3). For the magnification at which the pictures were taken, it seems to be impossible to tell them apart based on the microstructural features. It is important to point out that both powders exhibited similar particle size distribution (Table 1) and in-flight particle characteristics (Table 2), which probably favoured the formation of similar microstructures. This is an important characteristic to verify the role of the structural character of the feedstock powder on the coating properties, i.e., it will be possible to verify if the nanostructural character of the powder does make a difference in the wear performance.

3.4. Dry-sliding wear testing

3.4.1. Wear performance

Table 3 shows porosity, microhardness, crack propagation resistance and wear data of the coatings. The dry-sliding wear resistance characteristics of the FS and HVOF-sprayed coatings produced from the Nano powder stand out. Using a weighing balance (0.1 mg precision), it was not possible to observe a difference in mass (i.e., a mass loss) for the FS coating after wear testing; moreover, the mass loss of the HVOF-sprayed coating was almost negligible (Table 3). Therefore, these two coatings produced from a Nano powder exhibited the lowest volume loss and wear

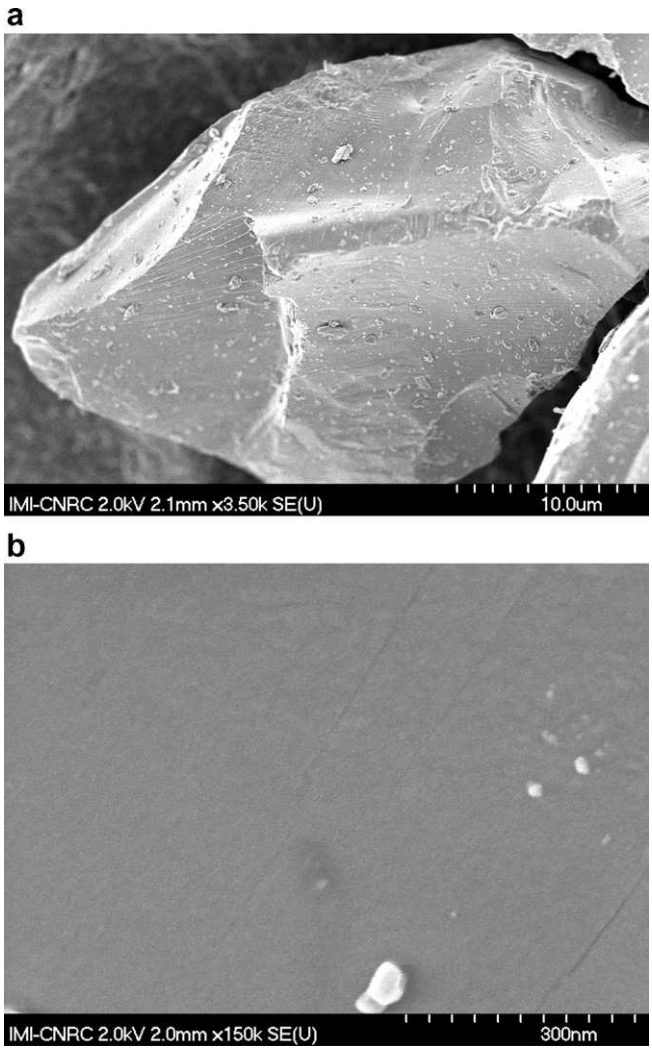

Fig. 3. (a) Fused and crushed (F&C) titania powder. (b) Higher magnification view of (a) showing the absence of ultrafine character.

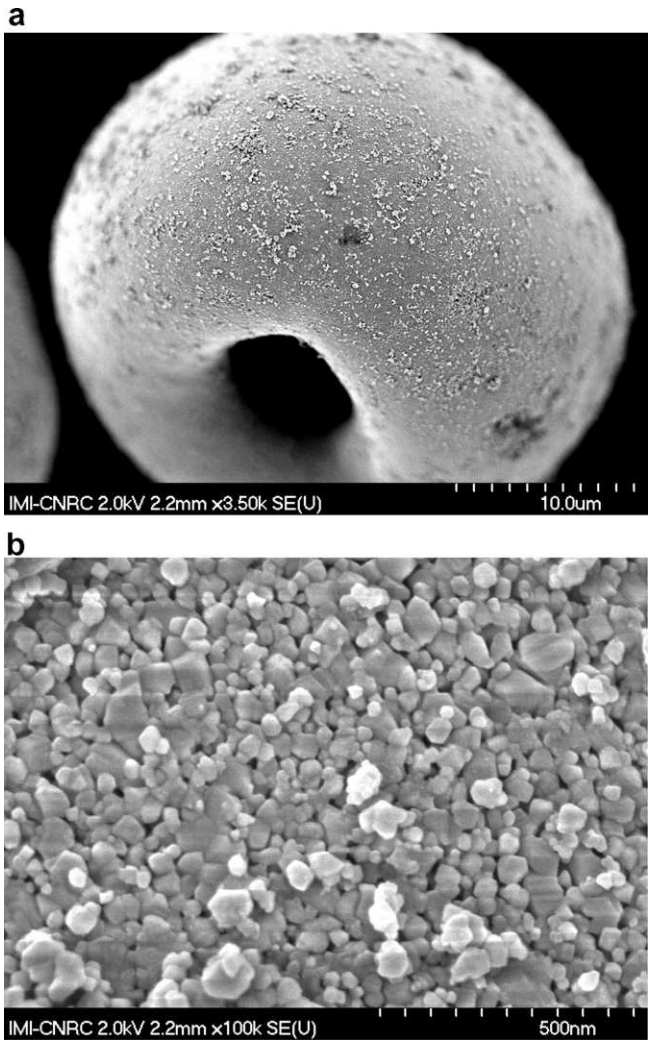

Fig. 4. (a) Nano spray-dried titania powder. (b) Higher magnification view of (a) showing the nanostructure of the agglomerate.

rate values, i.e., the highest dry-sliding wear resistance of all coatings tested in this study (Table 3). It is important to point out that the FS coating made from the Nano powder was tested two times. During the first test, it was also not possible to measure any significant mass loss, however, as the ruby broke during testing, the result was not counted in this paper.

As previously stated in Section 1.2 and Section 2.1, one of the objectives of this work was to verify if the powder morphology would influence the wear behaviour of these coatings. To accomplish this objective, the PF powder of Fig. 2 had been synthesized from an experimental spray-dried powder that exhibited ultrafine characteristics (Fig. 1) similar to those of the Nano powder (Fig. 4). During the PF processing (plasma-fusing), the powder of Fig. 1 lost part of the original ultrafine character (Fig. 2). Despite the differences in structure, the PF (Fig. 2) and Nano (Fig. 4) powders exhibited similar particle size distributions (Table 1) and both were HVOF-sprayed by developing spray parameters that would impart similar in-flight particle characteristics (i.e., temperature and velocity) for the two materials (Table 2). By looking at the microstructure of both coatings (Fig. 6), it is evident that they exhibit similar characteristics (at the magnification at which the pictures were taken). All these steps were developed and followed carefully to try to separate the "true influence" of the morphology/character/structure of the powders on the wear properties of the coatings from other possible influences, such as, particle size and in-flight particle characteristics. By looking at Table 3, it is possible to notice that the HVOF-sprayed Nano coating exhibited a significant superior wear resistance when compared to that of the HVOF-sprayed PF coating. Therefore, the nanostructural character of the feedstock powder does make a difference (for the better) in the dry-sliding wear performance of these coatings. However, the DE of the Nano powder was only approximately half that of the PF.

A similar type of thinking could also be applied for the FS coatings. Based on (i) the microstructures of the F&C (Fig. 5a) and Nano

Table 2
Particle velocity, temperature and DE values for the coatings employed in this study

Powder/Torch	V (m/s)	T (°C)	DE (%)
F&C/HVOF	880 ± 105	2091 ± 219	~8
PF/HVOF	944 ± 113	2206 ± 169	~45
Nano/HVOF	896 ± 89	2072 ± 187	~24
F&C/FS	na	na	~65
Nano/FS	70–80	2750–2850	~80
F&C/APS	na	na	~65
Nano/APS	280–310	2400–2500	~68

na – not available.

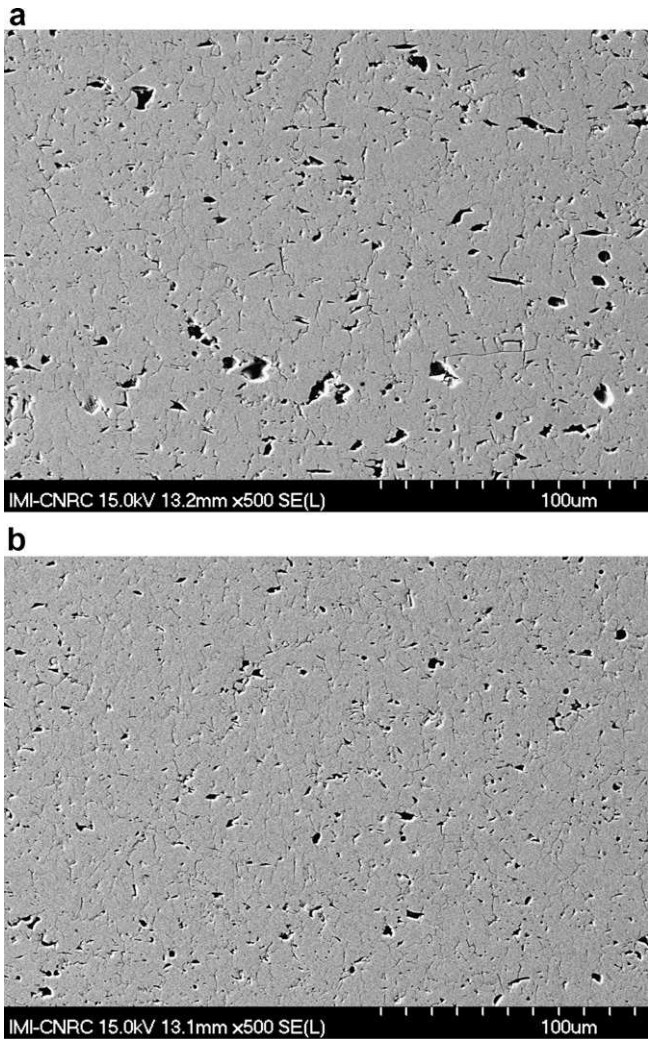

Fig. 5. Microstructures of the FS coatings produced from the following powders: (a) F&C and (b) Nano.

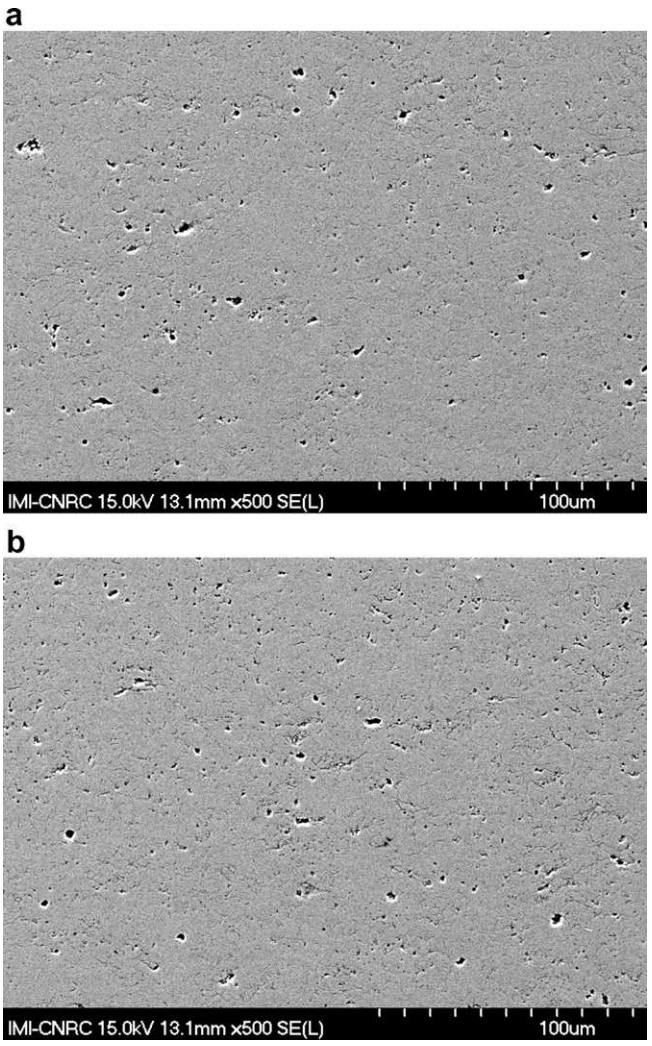

Fig. 6. Microstructures of the HVOF coatings produced from the following powders: (a) PF and (b) Nano.

(Fig. 5b) coatings, and (ii) their porosity and microhardness values (Table 3), it is difficult to explain why the wear resistance of the FS Nano coating was so superior to that of the FS F&C coating (Table 3). Therefore, the morphology of the Nano powder is probably playing a major role in the enhanced wear performance of this coating. Another factor that should be considered is the purity of the feedstock powder. The X-ray diffraction (XRD) pattern of the Nano powder shows only the presence of the stoichiometric phase TiO_2 [15], whereas, that of the F&C powder shows the presence of TiO_2 and a reduced phase (Ti_8O_{15} and Ti_7O_{13}) mixture [16].

One of the major factors that seems to be causing this difference in the wear properties of the coatings is the crack propagation resistance (Table 3), which has also been observed in previous works [3,4]. Vickers microhardness values of the coatings do not show significant differences (Table 3), even though the titania powders were thermally sprayed using different processing techniques (FS and HVOF), i.e., they were sprayed using significantly different particle temperature and velocity values (Table 2). Although the microhardness values are not available for the APS coating in Table 3, Vickers microhardness values of ~800–900 (300 gf) have been reported in the literature for F&C and Nano titania coatings deposited via APS [4,17]. Those values are in the range of those observed for the other coatings produced in this study.

When comparing coatings produced using the same processing techniques, i.e., HVOF or FS, the Nano coatings exhibited higher values of crack propagation resistance when compared to their

Table 3
Porosity, microhardness, crack propagation resistance and wear data of the coatings

Powder/Torch	Porosity (%) $n = 10$	HV (300 gf) $n = 10$	Crack propagation resistance (MPa $m^{1/2}$) (1 kgf) $n = 10$	Mass loss (g)	Volume loss (mm^3)
PF/HVOF	1.1 ± 0.2	859 ± 33	20.8 ± 4.4	0.0094	2.47
Nano/HVOF	1.0 ± 0.2	822 ± 40	25.6 ± 5.7	0.0008	0.21
F&C/FS	2.9 ± 0.3	849 ± 29	26.8 ± 3.4	0.0195	5.06
Nano/FS	2.0 ± 0.3	862 ± 20	38.8 ± 4.0	0.0000	0.00
F&C/APS	na	na	na	0.0053	1.29
Nano/APS	na	na	na	0.0136	na

na – not available.

counterparts (Table 3). It has to be stated again that the crack propagation resistance is not an absolute measure of fracture toughness. Nonetheless, crack propagation resistance is a useful technique to infer the "relative toughness" of coatings that (i) exhibit similar porosity and thickness levels and (ii) were deposited using the same type of thermal spray processing. Therefore, from Table 3 it can be inferred that the Nano coatings deposited via FS and HVOF tend to be tougher than the other ones deposited by the same processing techniques. Other works have also reported this tendency of higher crack propagation resistance levels offered by nanostructured-based ceramic oxide coatings [3,4,12,18–22,27].

Finally, it was observed that the two APS coatings exhibited a "moderate" dry-sliding wear resistance, particularly the coating produced from the Nano powder (Table 3). Due to the high temperatures of plasma jets (which are higher than those of HVOF and FS torches), it is hypothesized that the original nanostructure of the Nano powder may have been almost totally destroyed during coating deposition. Such an occurrence would eliminate major advantage of the nanostructural character of the feedstock and probably played a role in contributing to the poor wear performance.

3.4.2. Possible hypotheses to explain the higher crack propagation resistance levels

It is recognized that a deeper and more fundamental study would have to be carried out to link the origin of these higher crack propagation resistance levels exhibited by these coatings with the ultrafine character of the feedstock. This subject is beyond the scope of this work; however, this issue was extensively discussed in a review paper [3]. Researchers have proposed three mechanisms of toughening. One of the hypotheses employed to explain this enhanced crack propagation resistance (with some level of experimental evidence) is based on the crack arresting effect caused by the presence of dense semi-molten ultrafine agglomerates (pockets) embedded throughout the coating microstructure during thermal spraying. According to this hypothesis, dense pockets probably occur when the molten part of a semi-molten particle fully or almost fully infiltrates into the capillaries (porosity) of the ultrafine structure during thermal spraying [3].

The second hypothesis to explain the same behaviour (with some level of experimental evidence) is based on a better splat-to-splat contact achieved when using a nanostructured powder, which would also tend to impede crack propagation. Nanostructured particles (Fig. 4) exhibit larger surface areas when compared to those of the PF and F&C particles (Figs. 2 and 3, respectively). Therefore, the large surface area probably translates into a better capacity to absorb heat from the thermal spray jet.

In addition, the porous structure of the Nano powder (Fig. 4) could act as a thermal barrier so that the heat absorbed at the particle surface might propagate at lower rates towards the particle inner core when compared to those of F&C denser particles. This could lower the viscosity of the liquid phase of the agglomerate at its surface and lead to an improved splat-to-splat contact. Moreover, when compared to fully dense particles (e.g., F&C), an agglomerate of a given diameter would have a lower mass due to porosity; therefore a given amount of heat transfer could produce a higher temperature than in a denser particle of the same diameter, which also would tend to lower the particle viscosity at its surface. It has to be stressed that these two mechanisms of crack propagation arresting described above may work together [3]. The third hypothesis is based on the possibility of crack arresting by the presence of fine-pored agglomerates embedded in the coating microstructure. The pores would tend to hinder crack propagation [4]. It has to be pointed out that it was not identified in this research which of these three mechanisms is providing the higher crack propagation resistance levels of the FS and HVOF Nano-based coatings. It may be possible that all of them are working together simultaneously, but contribute to different degrees. For example, the major toughening mechanism for the HVOF Nano coating may not be the same as that of the FS Nano coating.

3.4.3. Dry-sliding wear scars: morphology

Analyzing the differences in wear scar morphologies exhibited by thermal spray coatings produced from Nano, F&C and PF ceramic oxide powders is an interesting way to better understand the behaviour of these coatings [3,19–28].

Figs. 7–11 show low and high magnification SEM pictures of the wear scars of the coatings tested in this study. It is important to point out that all sets of low and high magnification pictures were taken under the same conditions. This allows a better comparison of the wear mechanisms and performances exhibited by each coating. In general, two groups stand out. The first one is formed by the coatings produced from F&C or PF powders, deposited via FS (Fig. 7), APS (Fig. 9) and HVOF (Fig. 10). The wear scars of all these coatings exhibited brittle fracture, spallation/delamination and minor plastic deformation under sliding wear. The second group consists of the coatings produced from the Nano powder, either sprayed via FS (Fig. 8) or HVOF (Fig. 11). The wear scars of these coatings exhibit predominantly smooth features indicating higher degrees of plastic deformation when compared to those of the F&C and PF coatings. No significant spallation/delamination fea-

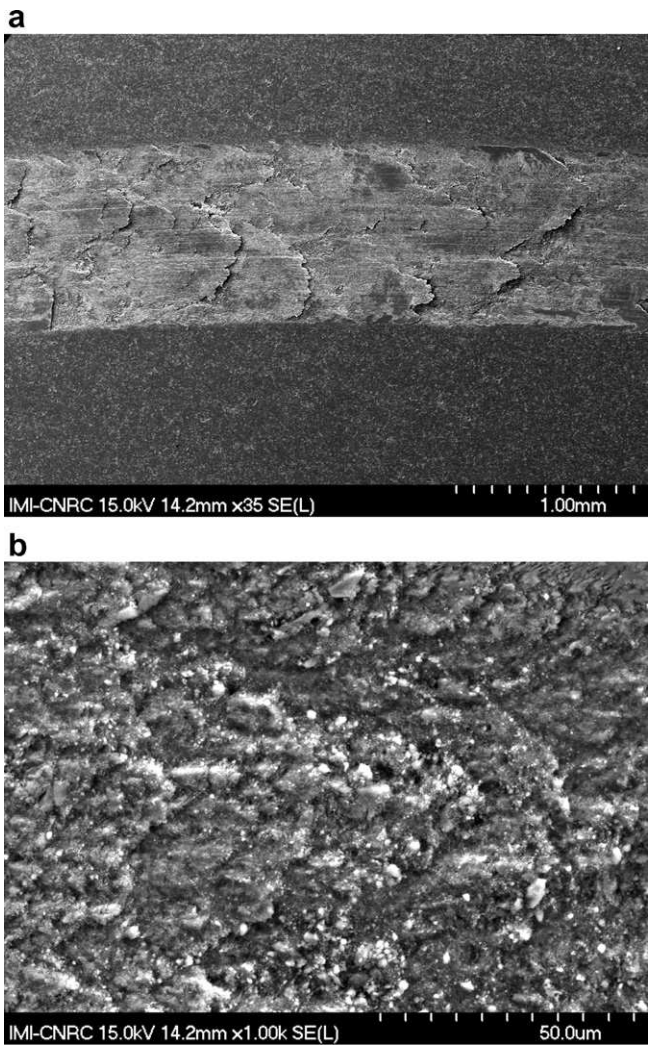

Fig. 7. (a) SEM micrograph of the wear scar on FS coating produced from the F&C powder. (b) Wear scar of (a) observed at higher magnification.

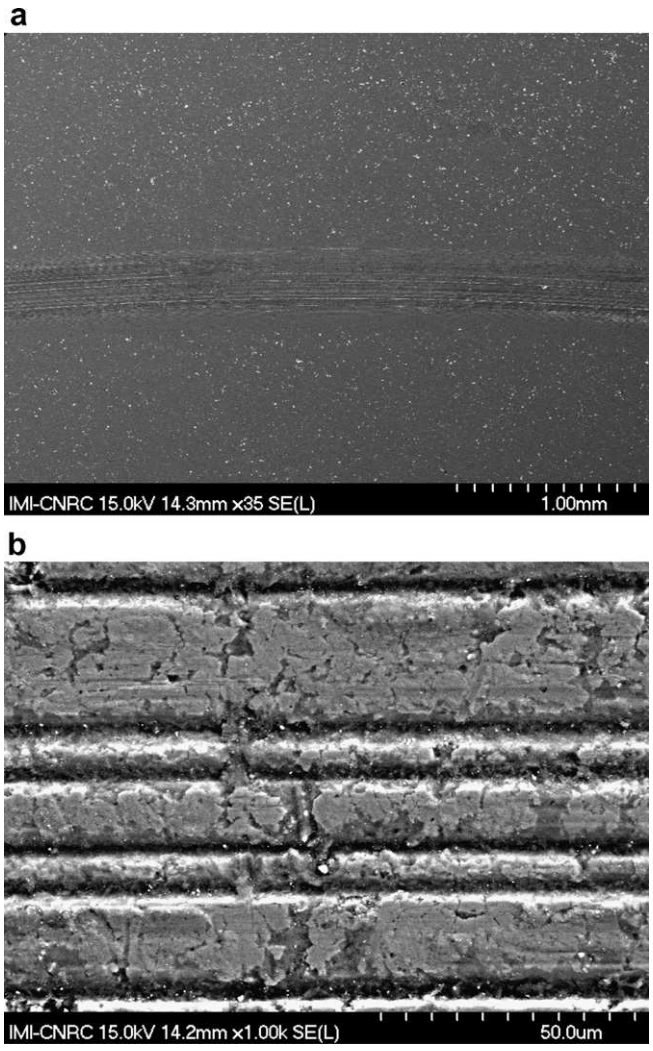

Fig. 8. (a) SEM micrograph of the wear scar on FS coating produced from the Nano powder. (b) Wear scar of (a) observed at higher magnification.

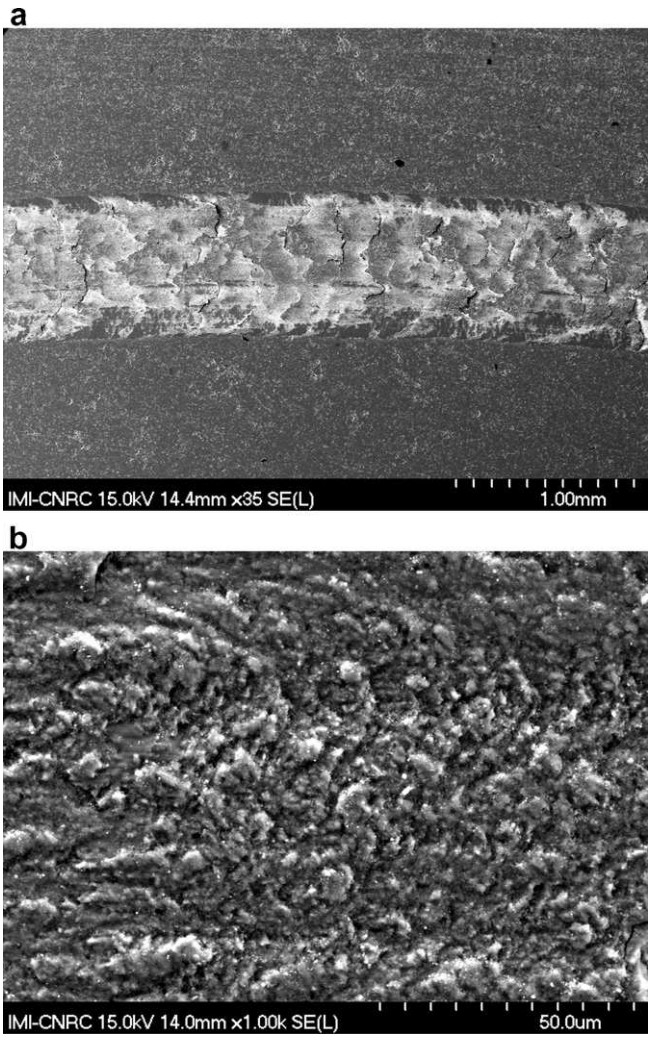

Fig. 9. (a) SEM micrograph of the wear scar on APS coating produced from the F&C powder. (b) Wear scar of (a) observed at higher magnification.

tures and irreversible deformation were observed for these coatings (Figs. 7, 9 and 10). It has to be stressed that some of these characteristics related to the wear scars of these types of ceramic oxide coatings have already been reported in previous works [3,20,24,26].

Plastic deformation (i.e., ductile flow) and fragmentation (i.e., brittle fracture) occur during the sliding wear of ceramic materials [8,19,24,26,29,30]. During the wear of a ceramic material, a transition of material removal mechanism from ductile mode to brittle mode occurs. The initial ductile flow progressively changes to brittle fracture after a critical depth of cut is reached. It has been reported that the critical depth of cut of a ceramic material is directly proportional to the square of its toughness-to-hardness ratio [31].

By looking at Table 3 it is possible to observe that the Vickers microhardness values of the coatings tested in this study are found in a range of 800–900 (300 gf), i.e., they are similar. However, the crack propagation resistance values of the Nano coatings sprayed by FS and HVOF tended to be higher than those of their counterparts (Table 3). As previously discussed in Section 3.4.1, from crack propagation resistance values it can be inferred that the Nano coatings tend to be tougher than the other ones (Table 3).

3.4.4. Dry-sliding wear scars: plasticity

As discussed in the previous section, the Nano coatings tend to be tougher than the other ones and all coatings exhibit similar hardness values. Therefore, it can be hypothesized that the critical depth of cut (toughness-to-hardness ratio) levels of the Nano coatings are higher than those of the other samples, i.e., the Nano coatings are able to exhibit higher plastic deformation capabilities. Consequently, the Nano coatings are able to withstand the same degree of mechanical loading and stress without exhibiting significant fracture and delamination, which helps to explain the formation of smooth wear scars and improved dry-sliding wear resistance of these coatings, i.e., this hypothesis agrees with the microstructural features of the wear scars of the Nano (Figs. 8 and 11), F&C (Figs. 7 and 9) and PF (Fig. 10) coatings.

To further explore this plasticity issue it is necessary to apply the concept of tribofilm. According to Bolelli et al. [8,19], the ability to form a smooth and compact surface film (i.e., tribofilm) by local plastic deformation is the key property determining coating performance in sliding wear. The tribofilm, which protects underlying material, is formed by plastically deformed splats and wear debris, which are caused by high local contact pressures and temperatures. The high local temperatures would be generated by friction and poor conductivity of ceramic materials.

According to Xie and Hawthorne [29,30], despite the fact that no complete elastic/plastic model has been developed for the wear caused by the sliding of a spherical indenter on a material's surface, it is reasonable to argue that a hydrostatic compressive stress is formed just below the contact surface of a rigid spherical indenter

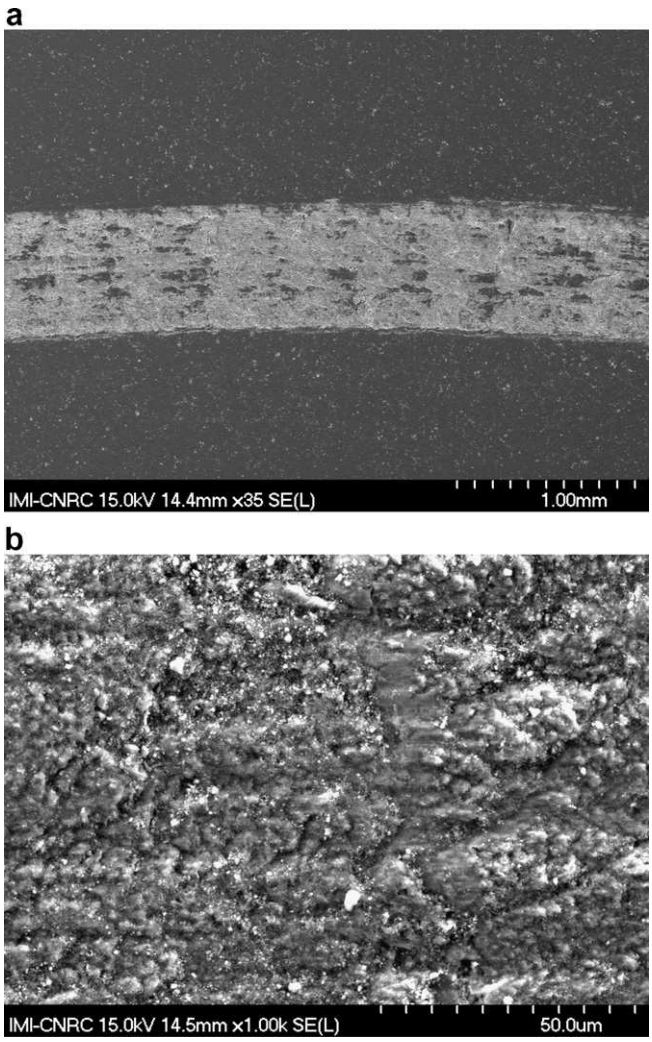

Fig. 10. (a) SEM micrograph of the wear scar on HVOF coating produced from the PF powder. (b) Wear scar of (a) observed at higher magnification.

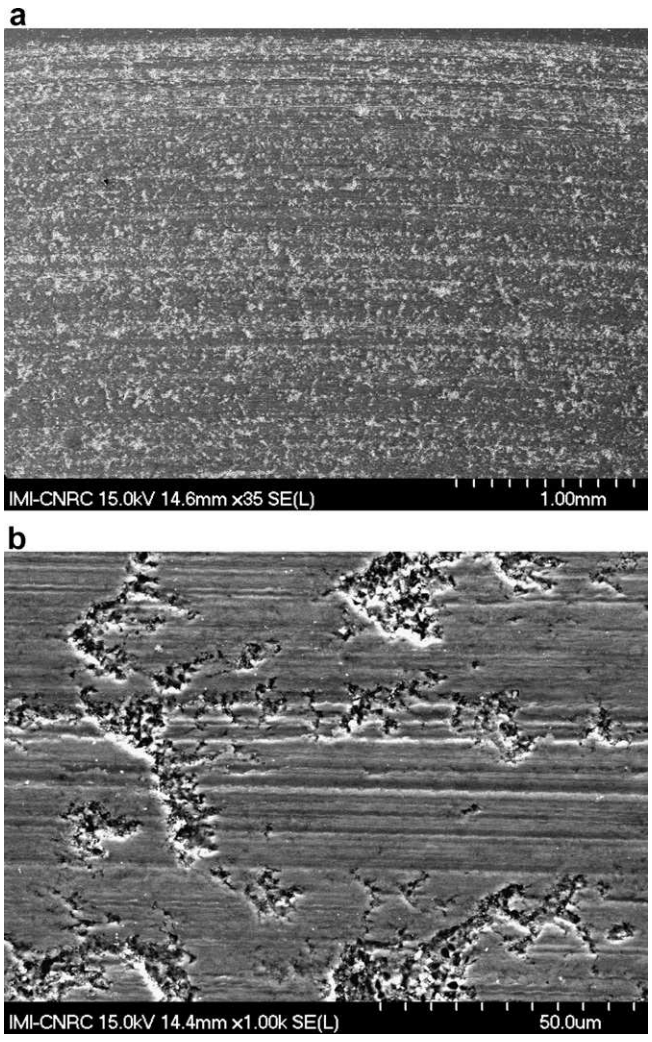

Fig. 11. (a) SEM micrograph of the wear scar on HVOF coating produced from the Nano powder. (b) Wear scar of (a) observed at higher magnification.

(e.g., between the ruby ball and coating), following the trends of an elastic–plastic indentation. In this type of elastic/plastic behaviour, the surface contact of the rigid indenter is encased in a semi-spherical core. Within this core there is a hydrostatic compressive stress that is equal to the hardness of the surface, which is surrounded by a plastic zone where the stresses and strains gradually decrease. Finally, this plastic zone is surrounded by an elastic region. According to Xie and Hawthorne [29,30], the work of Bridgeman [32] (and subsequently others), has shown that under sufficiently high hydrostatic pressures, brittle ceramic materials may be prevented from cracking so that any permanent deformation is essentially plastic. Therefore, the localized compression under a rigid indenter (e.g., ruby ball), aided by high local temperature generated during wear testing, may be high enough to prevent brittle failure, thereby allowing plastic deformation and the formation of smooth wear tracks, such as those observed in Figs. 8 and 11 for the Nano coatings.

Xie and Hawthorne [29,30] cited the works of Lawn [33] and Fischer-Cripps and Lawn [34] to explain that in bulk, sintered ceramics, plastic deformation in confined compression occurs predominantly via dissipative slip of "shear faults", i.e., weak particle/matrix interfaces or twin planes, rather than dislocation slip. This irreversible deformation can be described as "quasi-plastic" [33,34]. However, the plastic deformation mechanisms in thermally sprayed ceramic coatings would tend to be different because of their unique microstructures. Thermally sprayed ceramic coatings typically exhibit a randomly stacked splat/lamellar anisotropic microstructure with a network of intra- and inter-lamellar microcracks, which together with well-defined splat boundaries are sources of "shear faults" for "quasi-plastic" deformation. These concepts were also employed by Bolelli et al. [8,19] to explain differences in wear behaviour among ceramic thermal spray coatings.

3.4.5. Dry-sliding wear scars: resilience

Despite the fact that the tribofilm protects the underlying material from severe wear and forms a smooth wear scar, it has to be stressed that it does not impede material removal during wear. Xie and Hawthorne [29,30] observed smooth wear tracks that exhibited measurable material removal. Ridges along these wear scar tracks were also observed. However, the FS and HVOF-sprayed Nano coatings tested in this study exhibited insignificant material removal (Table 3), smooth wear scars with no ridges along the tracks and negligible irreversible deformation (Figs. 8 and 11). Therefore, there should be another factor affecting the performance of these two coatings.

An important property of a material is its ability to absorb energy when it is deformed without fracture or plastic flow, i.e., resilience. A resilient material can absorb energy by straining

elastically and this stored energy per unit volume is recoverable if the applied forces are reduced to zero. The FS and HVOF-sprayed Nano coatings of this study did not show significant signs of mass/volume loss, fracture or plastic flow (no ridges along the wear scars), and no significant irreversible deformation. Therefore, it can be considered that they exhibit high levels of resilience.

It is interesting to observe that the FS and HVOF-sprayed Nano coatings exhibited different characteristics of resilience. By looking at the low magnification pictures of the wear scars of all coatings (Figs. 7a–11a), it is possible to observe that the FS Nano coating (Fig. 8a) exhibits the narrowest wear scar (~0.4 mm), whereas, the HVOF Nano coating (Fig. 11a) exhibits the widest one (~2.5 mm). The ruby ball does not wear significantly the FS Nano coating (Fig. 8), which also induces a minimum wear on the ruby ball surface.

The ruby ball does also not wear significantly the HVOF Nano coating (Fig. 11), however, after the wear testing it is possible to observe that the ruby ball surface was flattened, i.e., severely worn off (Fig. 12).

In a tribological coupling between two different surfaces (materials), it is the basic principle that the harder one wears the softer one [8]. Alumina-based materials (9 Mohs), such as the ruby ball, are known to be harder than titania (5–6.5 Mohs). Despite that, when the worn off surface of the ruby ball is observed at higher SEM magnifications (Fig. 12b), it is possible to observe the typical characteristics of brittle fracture also exhibited by the wear scars of the F&C (Figs. 7b and 9b) and PF (Fig. 10b) coatings. Further analysis will have to be carried out to explain this phenomenon, which is beyond the scope of this current work.

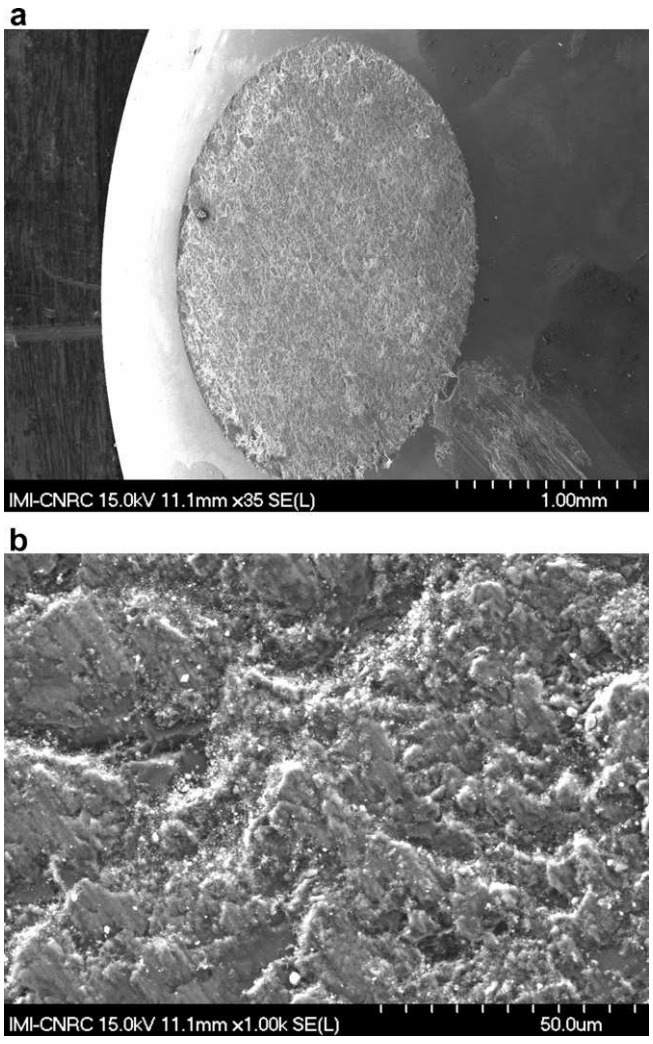

Fig. 12. (a) SEM micrograph of the worn off surface of the ruby ball used to test the HVOF coating produced from the Nano powder of Fig. 11. (b) Worn off surface of the ruby ball observed at higher magnification.

3.4.6. Dry-sliding wear scars: grinding and polishing

It has to be pointed out that this higher capability of forming smooth tribofilms exhibited by the Nano coatings (Figs. 8 and 11) may indicate that they can be easier to grind and polish, when compared to F&C (Figs. 7 and 9) and PF (Fig. 10) coatings. In the majority of the dry-sliding wear applications it is necessary to grind and polish the as-sprayed coatings prior to use. The process of grinding and polishing a ceramic coating can be expensive and time consuming, therefore if this process is facilitated, significant economy of energy and grinding/polishing materials may be achieved.

3.5. Integrity of the nanostructural character of the powder

The integrity of the nanostructural character of the powder during thermal spraying is a factor to be discussed in this type of research. One may argue if the nanostructural structure of the feedstock powder (Fig. 4) was totally destroyed during thermal spraying, due to the particle temperatures reported (Table 2), which are higher than that of the melting point of TiO_2, i.e., 1855 °C [9]. It has to be stressed again that a pyrometer-based device was used to measure particle temperature, consequently, the temperatures measured represented only the temperature at the particle surface, i.e., inner particle temperature levels were probably lower than the values reported in Table 2. When the fracture surface (cross-section) of the FS Nano coating is observed via SEM at higher magnifications (Fig. 13), it is possible to distinguish the presence of semi-molten ultrafine particles embedded in the coating microstructure, i.e., part of the original feedstock structure was preserved. It is important to point out that the molten part of the feedstock particles tended to penetrate into the capillaries (porosity) of the agglomerates.

Gell et al. [20] also observed these microstructural characteristics via SEM and transmission electron microscopy for APS nanostructured alumina–titania coatings. Therefore, despite the high temperatures of plasma-sprayed particles, part of the ultrafine structure of the feedstock was preserved in the microstructure of the coating, which also exhibited improved wear resistance. However, as the amount of semi-molten particles embedded in the coating microstructure was not quantified, it is not possible to infer how efficient they were in improving the crack propagation resistance of this coating and its wear performance. In fact, the major toughening mechanism for this specific coating may have been related to an improved splat-to-splat contact (and not crack arresting by dense semi-molten particles), due to a lower particle viscosity level at their surfaces, as discussed in Section 3.4.2 and reported in a review paper on this subject [3]. Further analysis will have to be carried out to better understand the role of the Nano-based feedstock on the improvement in wear properties of these specific coatings.

3.6. Isotropic behaviour of flame-sprayed nanostructured titania coating

When bulk, sintered ceramics are indented using Vickers indentation, depending on the indentation load and material properties, four major cracks tend to be observed originating at or near the corners of the Vickers indentation impression [5]. This phenomenon occurs due to the typical isotropic microstructure of bulk ceramics. Thermal spray coatings are known to exhibit anisotropic

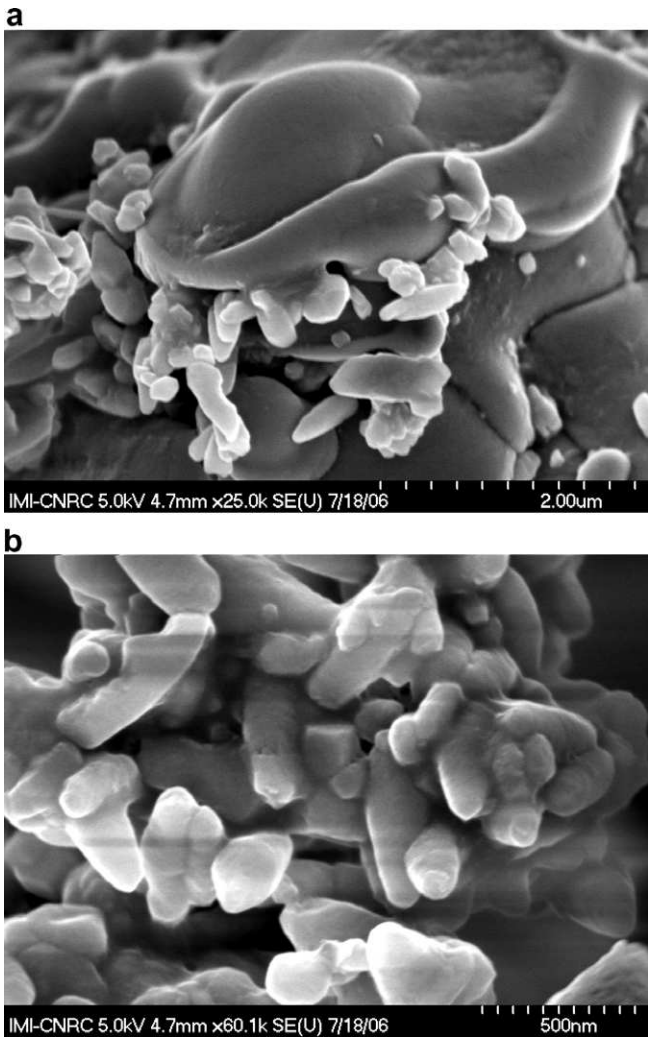

Fig. 13. (a) SEM micrograph of the fracture surface (cross-section) of the FS Nano coating showing the ultrafine structure of a semi-molten particle embedded in the coating microstructure by the action of a previously molten particle. (b) Another semi-molten particle embedded in the coating microstructure.

lamellar microstructures. Therefore, when thermally sprayed ceramic-based coatings are indented on the cross-section via Vickers indentation, with the indenter aligned such that one of its diagonals is parallel to the substrate surface, two major cracks parallel to the substrate surface may be observed originating at or near the corners of the Vickers indentation impression [3,8,35]. This anisotropic crack propagation occurs predominantly due to the well-defined lamellar boundaries, which provide easy crack propagation paths.

However, the FS Nano coating tested in this study tended to exhibit isotropic crack propagation under Vickers indentation, i.e., four major cracks with similar lengths were observed originating near or at the corners of the Vickers indentation impression, as shown in Fig. 14.

This isotropic phenomenon of crack propagation had been observed before for nanostructured-based titania coatings sprayed via HVOF [3] and APS [36], however, the particle size distribution of the nanostructured agglomerates varied from 5 to 20 μm, instead of the larger nanostructured agglomerates used in this work (Table 1). It is important to point out that the HVOF-sprayed Nano coating (Fig. 6b) did not exhibit this isotropic behaviour.

This isotropic crack propagation is not a typical characteristic of thermal spray coatings. It is shown in this work as a factor that may have contributed to the excellent dry-sliding wear performance of the FS Nano coating. Further investigation will be necessary to demonstrate the origin of this isotropic behaviour and if it is making an important influence on the mechanical performance of this coating under sliding wear.

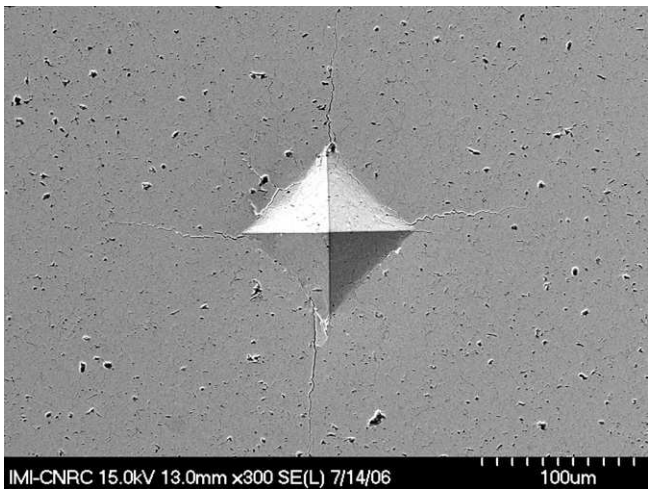

Fig. 14. Four major cracks with similar lengths were observed originating near or at the corners of the Vickers indentation impression on the cross-section of FS Nano titania coating.

4. Conclusions

In this work, nanostructured (Nano), fused & crushed (F&C) and plasma-fused (PF) titania (TiO_2) powder particles were thermally sprayed via FS, APS and HVOF processing techniques. The dry-sliding wear behaviour of these coatings was evaluated via ball-on-disk testing. The following conclusions were drawn:

- The FS coating produced from the Nano powder was the best performing of all coatings tested, exhibiting negligible mass/volume loss after sliding wear testing and DE values of ~80%.
- The volume loss of the HVOF-sprayed PF coating after sliding wear was ~12 times higher than that of the HVOF-sprayed Nano coating. The PF powder was initially produced from a spray-dried agglomerate that exhibited ultrafine structure, which was partially lost during the PF manufacture processing via plasma-fusing. Both PF and Nano powders exhibited similar overall particle size distribution and were sprayed using similar in-flight particle characteristics (i.e., temperature and velocity values). Both coatings exhibited similar microstructures and porosity levels. Therefore, these series of results show that the superiority in wear performance of the HVOF-sprayed Nano coating was highly dependent on the powder structure.
- The superior dry-sliding wear resistance of the FS and HVOF Nano coatings can be (partially) explained by their higher toughness levels (inferred from crack propagation resistance values), formation of a plastic and smooth tribofilm underneath the ruby ball on the coating surface, and high resilience.
- FS processing is the most affordable thermal spray technique to spray ceramic powders. It also has the lowest maintenance and operational costs, it is portable and exhibits the lowest energy consumption levels when compared to techniques like APS and HVOF. Based on these characteristics and on the wear results and DE values observed in this work, it is concluded that flame spraying Nano titania powders may become a very interesting alternative to produce coatings for dry-sliding wear applications.

Acknowledgements

This work could not have been carried out without the dedication, interest and vision of Mr. M. R. Dorfman (Sulzer Metco (US) Inc.) in seeking new alternatives in thermal spraying. His support was deeply appreciated. The authors also would like to thank Mr. C. Perdikaris and Dr. A. Sharma (Sulzer Metco (US) Inc.) for fruitful discussions about this research work.

References

[1] Thermal Spray Materials Guide, Sulzer Metco Inc., issued February 2006, AP-51, PDF file, July 30, 2007. www.sulzermetco.com/en/DesktopDefault.aspx/tabid-1740//3392_read-5304.
[2] Metco 102 Titanium Dioxide Powder, Technical Bulletin #10-092, issued October 2000, PDF file, Sulzer Metco Inc.
[3] Lima RS, Marple BR. Thermal spray coatings engineered from nanostructured ceramic agglomerated powders for structural, thermal barrier and biomedical applications: a review. J Therm Spray Technol 2007;16(1):40–63.
[4] Kim GE, Walker J. Successful application of nanostructured titanium dioxide coating for high-pressure acid-leach application. J Therm Spray Technol 2007;16(1):34–9.
[5] Anstis GR, Chantikul P, Lawn BR, Marshall DB. A critical evaluation of indentation techniques for measuring fracture toughness: I. Direct crack measurements. J Am Ceram Soc 1981;64(9):1073–82.
[6] Jacobs L, Hyland MM, De Bonte M. Study of the influence of microstructural properties on the sliding-wear behavior of HVOF and HVAF sprayed WC-cermet coatings. J Therm Spray Technol 1999;8(1):125–32.
[7] Shipway PH, McCartney DG, Sudaprasert T. Sliding wear behavior of conventional and nanostructured HVOF sprayed WC-Co coatings. Wear 2005;259:820–7.
[8] Bolelli G, Cannilo V, Lusvarghi L, Manfredini T. Wear behavior of thermally sprayed ceramic oxide coatings. Wear 2006;261:1298–315.
[9] Miyayama M, Koumoto K, Yanagida H. Engineering properties of single oxides. In: Schneider SJ, editor. Engineered materials handbook. Ceramics and glasses, vol. 4. Materials Park, OH, USA: ASM International; 1991. p. 748–57.
[10] Lima RS, Marple BR. High Weibull modulus HVOF titania coatings. J Therm Spray Technol 2003;12(2):240–9.
[11] Lima RS, Marple BR. Optimized HVOF titania coatings. J Therm Spray Technol 2003;12(3):360–9.
[12] Turunen E, Varis T, Gustafsson TE, Keskinen J, Falt T, Hannula S-P. Parameter optimization of HVOF sprayed nanostructured alumina and alumina–nickel composite. Surf Coat Technol 2006;200:4987–94.
[13] Kulkarni A, Gutleber J, Sampath S, Goland A, Lindquist WB, Herman H, Allen AJ, Dowd B. Studies of the microstructure and properties of dense ceramic coatings produced by high-velocity oxygen-fuel combustion spraying. Mater Sci Eng A 2004;369:124–37.
[14] Bolelli G, Lusvarghi L, Manfredini T, Pighetti Mantini F, Polini R, Turunen E, Varis T, Hannula S-P. Comparison between plasma- and HVOF-sprayed ceramic coatings. Part I: microstructure and mechanical properties. Int J Surf Sci Eng 2007;1(1):38–61.
[15] Gaona M, Lima RS, Marple BR. Nanostructured titania/hydroxyapatite composite coatings deposited by high velocity oxy-fuel (HVOF) spraying . Mater Sci Eng A 2007;458:141–9.
[16] Lima RS, Marple BR. NRC-IMI technical report #2003-102831-C CNRC, 2004.
[17] Lima RS, Marple BR. From APS to HVOF spraying of conventional and nanostructured titania feedstock powders: a study on the enhancement of the mechanical properties. Surf Coat Technol 2006;2006:3428–37.
[18] Lin X, Zheng Y, Lee SW, Ding C. Characterization of alumina–3 wt% titania coating prepared by plasma spraying of nanostructured powders. J Eur Ceram Soc 2004;24:627–34.
[19] Bolelli G, Lusvarghi L, Manfredini T, Pighetti Mantini F, Turunen E, Varis T, Hannula S-P. Comparison between plasma- and HVOF-sprayed ceramic coatings. Part II: tribological behavior. Int J Surf Sci Eng 2007;1(1):62–79.
[20] Gell M, Jordan EH, Sohn YH, Goberman D, Shaw L, Xiao TD. Development and implementation of plasma sprayed nanostructured ceramic coatings. Surf Coat Technol 2001;146–145:48–54.
[21] Ahn J, Hwang B, Song EP, Lee S, Kim NJ. Correlation of microstructure and wear resistance of Al_2O_3–TiO_2 coatings plasma sprayed with nanopowders. Metall Mater Trans A 2006;37A:1851–61.
[22] Tao S, Liang B, Ding C, Liao H, Coddet C. Wear characteristics of plasma-sprayed nanostructured yttria partially stabilized zirconia coatings. J Therm Spray Technol 2005;14(4):518–23.
[23] Li JF, Liao H, Wang XY, Normand B, Ji V, Ding CX, Coddet C. Improvement in wear resistance of plasma sprayed yttria stabilized zirconia coating using nanostructured powder. Tribol Int 2004;37:77–84.
[24] Chen H, Ding C, Zhang P, La P, Lee SW. Wear of plasma-sprayed nanostructured zirconia coatings against stainless steel under distilled-water conditions. Surf Coat Technol 2003;173:144–9.
[25] Chen H, Lee S, Zheng X, Ding C. Evaluation of unlubricated wear properties of plasma-sprayed nanostructured and conventional zirconia coatings by SRV tester. Wear 2006;260:1053–60.
[26] Chen H, Zhang Y, Ding C. Tribological properties of nanostructured zirconia coatings deposited by plasma spraying. Wear 2002;253:885–93.
[27] Jordan EH, Gell M, Sohn YH, Goberman D, Shaw L, Jiang S, Wang M, Xiao TD, Wang Y, Strutt P. Fabrication and evaluation of plasma sprayed nanostructured alumina-titania coatings with superior properties. Mater Sci Eng A 2001;301:80–9.
[28] Song EP, Ahn J, Lee S, Kim NJ. Microstructure and wear resistance of nanostructured Al_2O_3–8 wt% TiO_2 coatings plasma-sprayed with nanopowders. Surf Coat Technol 2006;201:1309–15.
[29] Xie Y, Hawthorne HM. The damage mechanisms of several plasma-sprayed ceramic coatings in controlled scratching. Wear 1999;233–235:293–305.
[30] Xie Y, Hawthorne HM. Wear mechanism of plasma-sprayed alumina coating in sliding contacts with harder asperities. Wear 1999;225–229:90–103.
[31] Liu X, Zhang B, Deng Z. Grinding of nanostructured ceramic coatings: surface observations and materials removal mechanisms. Int J Mach Tools Manufact 2002;42:1665–76.
[32] Bridgeman PW. Studies in large plastic flow and fracture. New York, NY, USA: McGraw-Hill; 1952.
[33] Lawn BR. Fracture of brittle solids. Cambridge, NY, USA: Cambridge University Press; 1993.
[34] Fischer-Cripps AC, Lawn BR. Stress analysis of contact deformation in quasi-plastic ceramics. J Am Ceram Soc 1996;79(10):2609–18.
[35] Ostojic P, McPherson R. Indentation toughness testing of plasma sprayed coatings. Mater Forum 1987;10(4):247–55.
[36] Moreau C, Bisson J-F, Lima RS, Marple BR. Diagnostics for advanced materials processing by plasma spraying. Pure Appl Chem 2005;77(2):443–62.